Journal of Computational and Applied Mechanics, Vol. 3., No. 1., (2002), pp. 93–101

VOLUME DEPENDENT STRENGTH OF POROUS MATERIALS AND STRUCTURES

Surot Thangjitham and Robert A. Heller
Department of Engineering Science and Mechanics
Virginia Tech, Blacksburg, Virginia, USA
thangjitham@vt.edu

[Received: April 6, 2002]

Dedicated to Professor Gyula Béda on the occasion of his seventieth birthday

Abstract. The size effects in reliability problems of porous materials and structures are considered in this study. The proposed analysis relies on a modified Weibull distribution with mean strength-volume relations obtained from experiments. The procedure is then applied to finite plates with circular holes of increasing diameters. Because of the nonlinearity of the stressed volume in the vicinity of the holes, the volume dependence of the strength becomes pronounced. The probability of survival of such plates is calculated and indicates a strong dependence on the stressed volume of the plate.

Mathematical Subject Classification: 74K20, 74M99, 74R99
Keywords: Weibull distribution, volume dependent, stress concentration, reliability analysis

1. Introduction

It is common knowledge that engineering materials are prone to size effects. Carefully prepared laboratory size specimens are usually stronger than full size structural components. This occurrence is especially true for brittle and porous materials such as ceramics and concrete. In previous studies, this phenomenon was treated on the basis of the Weakest Link Theory and the Weibull distribution [1-2]. According to the analysis, a component is assumed to be composed of a large number of elements (characteristic volume) of random strength that are connected in a series combination. The random variation of the element strength is mainly characterized by the number and geometry of initial flaws contained in the element. The failure of the component is assumed to occur when any one of the elements fails. The reliability of the component decreases, therefore, as the number of the elements (material volume) increases. Consequently, the reliability approaches unity as the volume of the material is reduced to zero and approaches zero as the volume increases. While this type of analysis gives reasonable results for intermediate size elements, it predicts an unlimited increase in strength as the volume approaches zero [3-8].

Recent researches have been focused on the development of mathematical models to predict size effects in materials [9-14]. Both micro- and macro-mechanical models have been proposed to relate material and geometrical parameters to size effects. However, no unified relation applicable to a large class of materials has yet been established. Instead, many empirical models have been used to extrapolate size effects in laboratory specimens to size effects in practical components.

A hyperbolic function has been used to define the size effect phenomenon [9-11] in ceramics and cementitious materials. Such a relationship assumes that the smallest volume is strongest while for large volumes the strength diminishes to zero. Observations on porous materials, however, indicate that strength does not increase monotonically for small volumes. As the volume approaches the size of the pores, its strength becomes weaker. A maximum strength, on the other hand, is observed for intermediate sizes, diminishing again to a nonzero value for structural components. As a result, a hyperbolic function for size effect, where strength is monotonically increasing with decreasing volume, is no longer applicable. To account for such observations, a modified size effect function is introduced and is used in the reliability analysis of porous structures.

2. **Size Effect Function**

The mean strength of a given volume v, $\bar{r}(v)$, is expressed in terms of the characteristic mean strength, $\bar{r}_c$, and the size effect function $\xi(\rho)$ as

$$\bar{r}(v) = \bar{r}_c \xi(\rho) \tag{2.1}$$

where $\rho = v/v_c$ is the volume ratio with v_c the characteristic volume of the material. Size effect is modelled as a combination of a classical hyperbolic relationship [11] and a Rayleigh type function

$$\xi(\rho) = \alpha_\infty + \frac{\alpha_1}{\sqrt{1+\beta_1 \rho}} + \alpha_2 \exp[-\beta_2 \left(\ln \rho - \gamma_2\right)^2] \tag{2.2}$$

with α_∞ the minimum value asymptotically approached for larger volumes, α_1 and β_1 the parameters for the classical hyperbolic size effect function, and α_2, β_2, and γ_2 the parameters for the Rayleigh type size effect function. These parameters characterize the size effects of materials such that

$$\lim_{\rho \to 0} \xi(\rho) = \alpha_\infty + \alpha_1 = \frac{\bar{r}_0}{\bar{r}_c} \qquad \text{(micro mean strength)} \tag{2.3}$$

$$\lim_{\rho \to \infty} \xi(\rho) = \alpha_\infty = \frac{\bar{r}_\infty}{\bar{r}_c} \qquad \text{(macro mean strength)} \tag{2.4}$$

$$\lim_{\rho \to 1} \xi(\rho) = \alpha_\infty + \frac{\alpha_1}{\sqrt{1+\beta_1}} + \alpha_2 e^{-\beta_2 \gamma_2^2} = 1 \qquad \text{(characteristic strength)} \tag{2.5}$$

where $\bar{r}_0$, $\bar{r}_\infty$, and $\bar{r}_c$ are the micro-, macro-, and characteristic mean strengths of materials, respectively.

For the purposes of illustration, the following coefficients $\alpha_\infty = 0.3587$, $\alpha_1 = 0.5380$, $\alpha_2 = 0.2690$, $\beta_1 = 0.2$, $\beta_2 = 0.3$, $\gamma_2 = 2$ are used. Figure 1 shows the variations of the size effect function $\xi(\rho)$ and of the hyperbolic function.

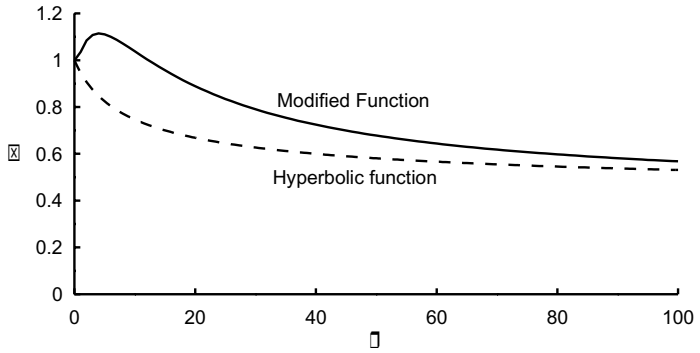

Figure 1. Size effect $\xi(\rho)$ as a function of volume ratio $\rho = v/v_c$.

The parameters in the above equations are obtained from experiments on specimens of various sizes where mean strength and dispersion (standard deviation) are measured. To analyze the reliability of a component with a given size, its mean strength is obtained from (2.2) and is then used in a two parameter Weibull distribution given as

$$f_R(r,\rho) = \frac{\eta}{\lambda}\left(\frac{r}{\lambda}\right)^{\eta-1} \exp\left[-\left(\frac{r}{\lambda}\right)^{\eta}\right] \tag{2.6}$$

where the parameters η and λ are obtained as

$$\frac{1}{\Gamma\left[1+\frac{1}{\eta}\right]^2}\left(\Gamma\left[1+\frac{2}{\eta}\right] - \Gamma\left[1+\frac{1}{\eta}\right]^2\right) - \delta^2 = 0\,, \tag{2.7}$$

$$\lambda(\rho) = \frac{\bar{r}_c \xi(\rho)}{\Gamma\left[1+\frac{1}{\eta}\right]} \tag{2.8}$$

where δ is the coefficient of variation and $\Gamma[.]$ is the gamma function.

The corresponding reliability function for a given level of induced stress, σ, is obtained as

$$L(\sigma,\rho) = \exp\left[-\left(\frac{\sigma}{\lambda}\right)^{\eta}\right] \tag{2.9}$$

As an illustration, a set of density functions, $f_R(r,\rho)$ is presented in Figure 2 for a characteristic mean strength, $\bar{r}_c = 30$ MPa, a coefficient of variation, $\delta = 0.2$ and various volume ratios, $\rho = v/v_c$. Figure 3 is a three dimensional plot of the density function $f_R(r,\rho)$. Reliability functions are plotted in Figure 4.

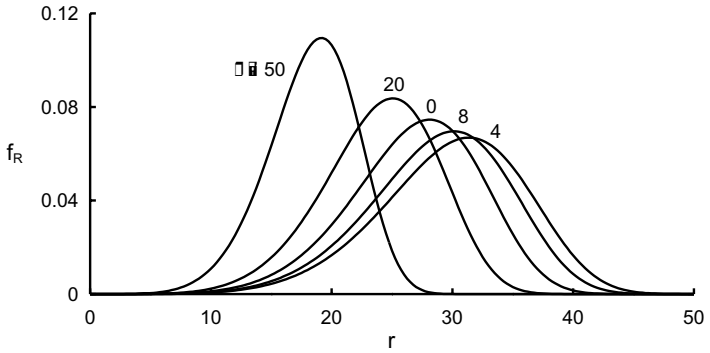

Figure 2. Probability densities $f_R(r,\rho)$ as functions of strength, r, for various volume ratios, ρ.

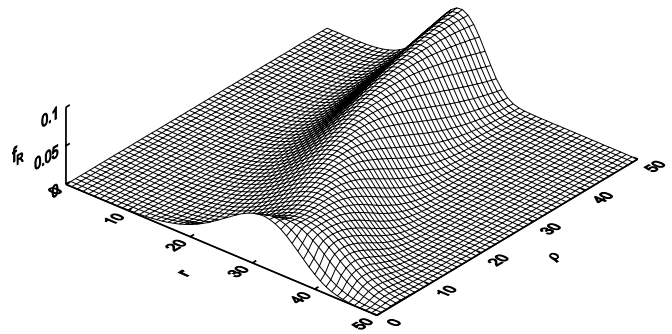

Figure 3. Variations of probability densities $f_R(r,\rho)$ as functions of strength, r, and volume ratio, ρ.

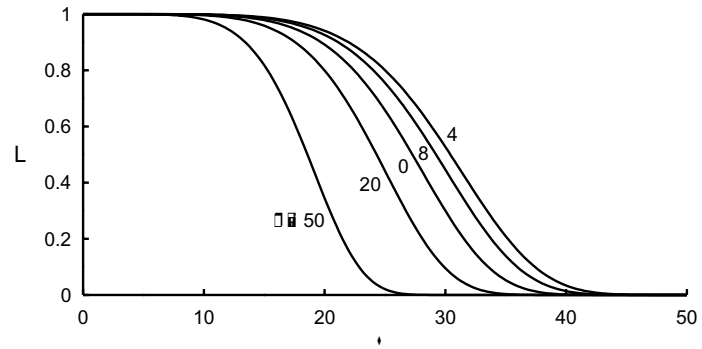

Figure 4. Reliabilities, $L(\sigma,\rho)$, as functions of applied stress, σ, for various volume ratios, ρ.

It is seen that the reliability of a component is volume dependent, first increasing and then decreasing with increasing volume. The reliabilities for a uniform plate

subjected to far-field applied uniform stress σ_0 along the x_2-direction (Figure 5 as $a \to 0$), are plotted in Figure 6 as functions of plate volume ratios ρ for various values of applied stress.

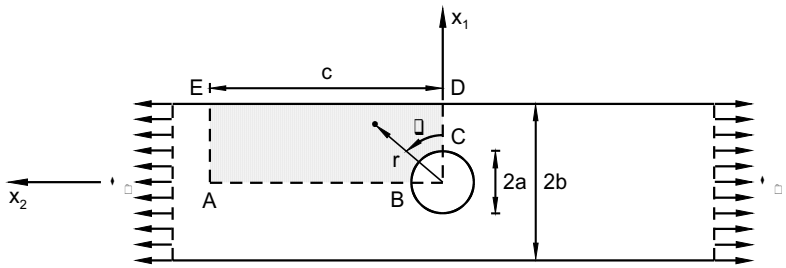

Figure 5. Plate geometry.

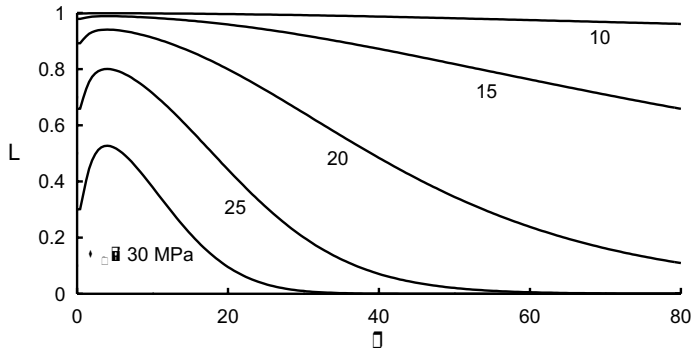

Figure 6. Reliabilities as functions of plate volume ratio, ρ, for various levels of applied stress σ_0.

3. **Analysis of Plates with Circular Holes**

Plates of unit thickness with various hole sizes, as shown in Figure 5, are analyzed. As the hole diameter is varied, the stressed volume of material in the vicinity of the hole also changes.

Stresses in terms of the stress functions, $\Phi(r,\theta)$, in polar coordinates (r,θ) are given by

$$\sigma_{rr}(r,\theta) = \frac{1}{r}\frac{\partial\Phi}{\partial r} + \frac{1}{r^2}\frac{\partial^2\Phi}{\partial\theta^2}, \tag{3.1}$$

$$\sigma_{\theta\theta}(r,\theta) = \frac{\partial^2\Phi}{\partial r^2}, \tag{3.2}$$

$$\sigma_{r\theta}(r,\theta) = -\frac{\partial}{\partial r}\left(\frac{1}{r}\frac{\partial\Phi}{\partial\theta}\right). \tag{3.3}$$

The general solution for the stress function

$$\Phi(r,\theta) = \phi_0 + \phi_1 e^{i\theta} + \sum_{n=1}^{\infty}\phi_n e^{in\theta} \tag{3.4}$$

where

$$\phi_0(r) = a_0 + b_0 \ln r + c_0 r^2 + d_0 r^2 \ln r\,, \tag{3.5}$$

$$\phi_1(r) = a_1 r + b_1 r^{-1} + c_1 r^3 + d_1 r \ln r\,, \tag{3.6}$$

$$\phi_n(r) = a_n r^{-n} + b_n r^{2-n} + c_n r^n + d_n r^{2+n} \tag{3.7}$$

with integration constants a_n, b_n, c_n, and d_n; $n = 0, 1, 2, \ldots$, to be evaluated by applying the proper boundary conditions.

For an infinite plate subjected to far-field uniaxial stress, σ_0, in the x_2-direction, equations (3.1)-(3.3) are reduced to

$$\sigma_{rr}(r,\theta) = \frac{1}{2}\sigma_0 \left[\left(1 - \frac{a^2}{r^2}\right) - \left(1 - 4\frac{a^2}{r^2} + 3\frac{a^4}{r^4}\right)\cos 2\theta \right], \tag{3.8}$$

$$\sigma_{\theta\theta}(r,\theta) = \frac{1}{2}\sigma_0 \left[\left(1 + \frac{a^2}{r^2}\right) + \left(1 + 3\frac{a^4}{r^4}\right)\cos 2\theta \right], \tag{3.9}$$

$$\sigma_{r\theta}(r,\theta) = \frac{1}{2}\sigma_0 \left(1 + 2\frac{a^2}{r^2} - 3\frac{a^4}{r^4}\right)\sin 2\theta\,. \tag{3.10}$$

The stress functions ϕ_n; $n = 0, 1, 2, \ldots$, for a semi-infinite plate (Figure 5), also loaded with far-field uniaxial stress σ_0, in the x_2-direction, satisfying the traction-free boundary conditions at the hole surface of radius a, are given as

$$\phi_0(r) = a_0 + b_0 \left(\ln r - \frac{r^2}{2a^2}\right), \tag{3.11}$$

$$\phi_1(r) = a_1 r + b_1 \left(\frac{a^4 + r^4}{a^4 r}\right), \tag{3.12}$$

$$\begin{aligned} \phi_n(r) \;=\; & a_n \left(r^{-n} - (n+1)\,a^{-2n} r^n + n a^{-2(n+1)} r^{n+2}\right) + \\ & b_n \left(r^{2-n} - (n+1)\,a^{-2(n-1)} r^n + n a^{-2n} r^{n+2}\right). \end{aligned} \tag{3.13}$$

It is noted that only two integration constants (a_n and b_n) remain to be determined by the traction-free boundary conditions on the free edges at $x_1 = \pm b$ and the far-field stress boundary conditions at $x_2 \to \infty$.

Because of symmetry of loading and plate geometry, the stress function is reduced to

$$\Phi(r,\theta) = \phi_0 + \sum_{n=2,4,6,\ldots}^{\infty} \phi_n(r)\, e^{in\theta}\,. \tag{3.14}$$

Depending on the level of accuracy required, the stress function is truncated to a finite number of N functions, ϕ_n; $n = 0, 1, 2, \ldots, N$. This leads to a total number of $2N + 1$ constants (a_0 is not required in the stress expressions) that need to be evaluated. To accomplish this, the method of least squared boundary collocation is used.

The rectangular stress components, σ_{11}, σ_{22}, and σ_{12} are obtained as

$$\sigma_{11}(r,\theta) = \frac{\sigma_{rr}+\sigma_{\theta\theta}}{2} + \frac{\sigma_{rr}-\sigma_{\theta\theta}}{2}\cos 2\theta - \sigma_{r\theta}\sin 2\theta\,, \tag{3.15}$$

$$\sigma_{22}(r,\theta) = \frac{\sigma_{rr}+\sigma_{\theta\theta}}{2} - \frac{\sigma_{rr}-\sigma_{\theta\theta}}{2}\cos 2\theta + \sigma_{r\theta}\sin 2\theta\,, \tag{3.16}$$

$$\sigma_{12}(r,\theta) = \frac{\sigma_{rr}-\sigma_{\theta\theta}}{2}\sin 2\theta + \sigma_{r\theta}\cos 2\theta\,. \tag{3.17}$$

The average normal stress in the net area $(b-a)$ is calculated as

$$\sigma_{\text{avg}} = \frac{1}{b-a}\int_a^b \sigma_{rr}(r,0)dr\,. \tag{3.18}$$

4. **Probability Analysis of Plates with Holes**

The stresses in semi-infinite plates with various widths $(2b)$ and hole sizes $(2a)$ have been calculated using (3.11)-(3.17). The average stress has also been obtained from (3.18). In order to examine the volume effects created by the presence of holes, average stresses were calculated for applied stresses σ_0 of 20 MPa and 25 MPa and their reliabilities were computed from (2.9).

The results are plotted in Figs. 7 and 8 as functions of the plate volume ratio ρ for several plate width to hole size ratios, b/a. The effective plate volume, v_e, per unit length along the x_2-direction, corresponding to a finite hole size is greater than the actual plate volume per unit length along the x_2-direction of the plate. This effective volume is given as

$$v_e = \kappa v \tag{4.1}$$

where the non-dimensional factor κ is computed using the average stress

$$\kappa = \frac{\sigma_{\text{avg}}}{\sigma_0}\,. \tag{4.2}$$

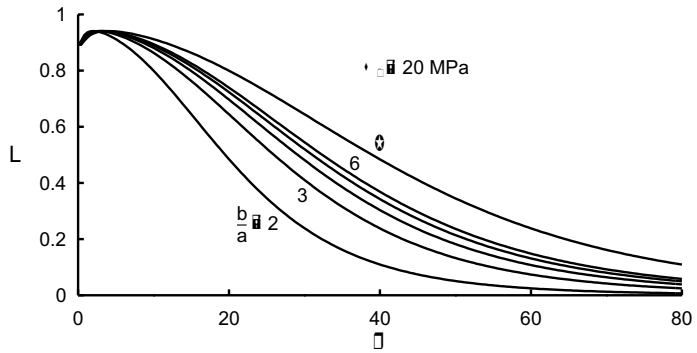

Figure 7. Reliabilities as functions of plate volume ratio, ρ, for various hole size ratios, b/a, subjected to applied stress $\sigma_0 = 20$ MPa

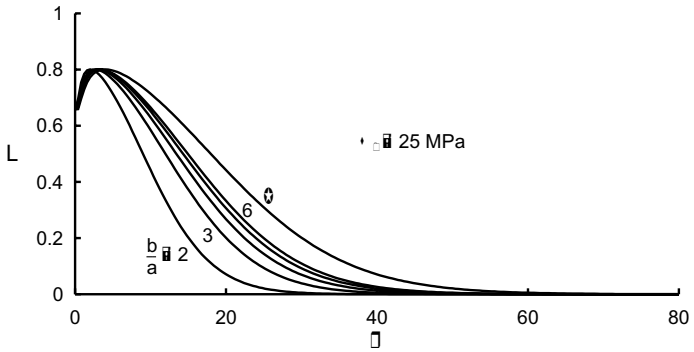

Figure 8. Reliabilities as functions of plate volume ratio, ρ, for various hole size ratios, b/a, subjected to applied stress $\sigma_0 = 25$ MPa

Table 1 presents the conventional stress concentration factor, $k = \sigma_{\max}/\sigma_0$ and the effective volume ratio κ.

Table 1. Stress concentration factor, k, and effective volume factor, κ, for various plate width to hole diameter ratios, b/a

	b/a					
	2	3	4	5	6	∞
k	4.141	3.444	3.224	3.133	3.082	3
κ	1.999	1.501	1.339	1.256	1.204	1

Because this effective volume, v_e, is greater than the actual volume, v, the size effect (larger size is weaker) is apparent. As the hole size ratio, b/a, increases, the curves approach the reliability function of a solid plate.

5. **Conclusions**

Experimentally observed size effects have been modelled by a modified hyperbolic function that indicates strength variations as a function of stressed volume. Applied to the reliability of porous materials, these reliability functions also show the effects of volume. The analysis of plates containing circular holes of various sizes indicates that as the plate width to hole diameter ratio increases, i.e., as the hole becomes smaller, the reliability of the plate increases. This is due to the fact that the critical stressed volume around the hole is also smaller. Experiments are needed in order to determine the coefficients of the size effect relationships.

REFERENCES

1. Weibull, W.: *A Statistical Theory of the Strength of Materials*, Proceedings of the Royal Swedish Institute for Engineering Research, No. 151, Stockholm, (1939).
2. Weibull, W.: *A Statistical Distribution Function of Wide Applicability*, ASME Journal of Applied Mechanics, 18, (1951), 293.

3. Davies, D. G.: *The Statistical Approach to Engineering Design of Ceramics*, Proceedings of the British Ceramic Society, 22, (1973), 429-452.
4. Stanley, P., Fessler, H. and Sivill, A. D.: *An Engineer's Approach to the Prediction of Failure Probability of Brittle Components*, Proceedings of the British Ceramic Society, 22, (1973), 453-487.
5. Trantina, G. G. and deLorenzi, H. G.: *Design Methodology for Ceramic Structures*, ASME Journal of Engineering for Power, 99 (4), (1977), 559-566.
6. Stanley, P. and Margetson, J.: *Failure Probability Analysis of an Elastic Orthotropic Brittle Cylinder Subjected to Axisymmetric Thermal and Pressure Loading*, International Journal of Fracture, 13, (1977), 787-806.
7. Margetson, J.: *Failure Probability Evaluation of an Anisotropic Brittle Structure Derived from a Thermal Stress Solution*, in Thermal Stresses in Severe Environments, D. P. H. Hasselman and R. A. Heller, eds., Plenum Press, New York, (1980), 503-519.
8. Heller, R. A., Thangjitham, S., and Yeo, I.: *Size Effects in Brittle Ceramics*, AIAA-90-113, Proceedings of the 31st AIAA/ASME/ASCE/ASC Structures, Structural Dynamics, and Materials Conference, Long Beach, CA, (1990).
9. Bažant, Z. P. and Kazemi, M. T.: *Size Effect in Fracture of Ceramics and Its Use to Determine Fracture Energy and Effective Process Zone Length*, Journal of American Ceramic Society, 73 (7), (1990), 1841-1853.
10. Mazars, J., Pijaudier-Cabot, G. and Saouridis, C.: *Size Effect and Continuous Damage in Cementitious Materials*, International Journal of Fracture, 51, (1991), 159-173.
11. Bažant, Z. P. and Planas, J.: *Fracture and Size Effect in Concrete and Other Quasibrittle Materials*, CRC Press, Boca Raton, Florida, (1997).
12. Hoshide, T. Murano, J. and Kusaba, R.: *Effect of Specimen Geometry on Strength in Engineering Ceramics*, Engineering Fracture Mechanics, 59 (5), (1998), 655-665.
13. Labuz, J. F. and Biolzi, L.: *Characteristic Strength of Quasi-Brittle Materials*, International Journal of Solids and Structures, 35, (31-32), (1998), 4191-4203.
14. Guinea, G. V., Elices, M. and Planas, J.: *Assessment of the Tensile Strength through Size Effect Curves*, Engineering Fracture Mechanics, 65, (2000), 189-207.